Scientific Research Publishing

Open Journal of Composite Materials, 2026, 16(4), 107-118
https://www.scirp.org/journal/ojcm
ISSN Online: 2164-5655
ISSN Print: 2164-5612

Characterization of Clay and Sand Bivalve (*Corbula trigona*) Shells for the Design of a Building Material

Boushia Syloé N'guettia[1], Soumahoro Gueu[1], Joseph Sei[2]

[1]Laboratory of Industrial Processes, Synthesis, Environment and Energy (ESCPE), Félix Houphouët-Boigny National Polytechnic Institute of Yamoussoukro (INP-HB), Yamoussoukro, Côte d'Ivoire
[2]Laboratory of Constitution and Reaction of Matter, Faculty of Sciences of Matter Structures and Technology, Félix Houphouët-Boigny University of Abidjan, Abidjan, Côte d'Ivoire
Email: syloefr2003@gmail.com

How to cite this paper: N'guettia, B.S., Gueu, S. and Sei, J. (2026) Characterization of Clay and Sand Bivalve (*Corbula trigona*) Shells for the Design of a Building Material. *Open Journal of Composite Materials*, **16**, 107-118.
https://doi.org/10.4236/ojcm.2026.164008

Received: August 3, 2026
Accepted: September 18, 2026
Published: September 21, 2026

Abstract

Portland cement is a high-performance construction material widely used in the building industry. However, its high cost and the environmental pollution associated with its production have prompted the search for cost-effective and environmentally friendly alternative materials. Several studies have investigated the use of bivalve shells (e.g., clams, mussels, and oysters) as partial or complete substitutes for Portland cement in construction materials. The aim of this study is to valorize *Corbula trigona* bivalve shells, clay, and sand for the development of a sustainable construction material. To this end, the clay and bivalve shells were ground to a particle size of 80 µm and calcined at 700˚C and 900˚C, respectively. The raw materials, together with the sand, were then characterized to evaluate their suitability for mortar production. The characterization results showed that the sand had a 0/4 particle-size distribution, a sand equivalent value of 85%, a bulk density of 1.54 g/cm^3, and a specific gravity of 2.55 g/cm^3. X-ray fluorescence (XRF) analysis revealed that the sand contained approximately 95 wt.% SiO_2. XRD and IR analysis show that the clay is mainly composed of kaolinite and the TGA/TGA curve on the bivalve shells shows that the formation of CaO from $CaCO_3$ ends at a temperature of about 800˚C, while the dehydroxylation of the clay ends at a temperature above 600˚C. These results highlight the potential of these raw materials for future mortar design.

Keywords

Bivalve Shells, *Corbula trigona*, Clay, Sand, Construction Materials

1. Introduction

A wide variety of construction materials are currently used for residential buildings worldwide, including wood, stone, steel, clay bricks, and concrete. Considerable research has been devoted to improving the mechanical performance and thermal comfort of these construction materials.

In Africa, particularly in Côte d'Ivoire, traditional construction materials are increasingly being replaced by Portland cement-based materials. Despite the high cost of cement and the growing number of cement manufacturing plants, domestic demand remains unmet.

Portland cement is a high-quality construction material that first appeared in the 1820s and is now one of the most widely used construction materials worldwide. Its continuously increasing production amounts to several billion tonnes annually. According to Folliet (2011), emerging countries account for approximately 90% of global cement consumption. Furthermore, the World Cement Association (WCA) reports that the cement industry is responsible for approximately 5% - 6% of global greenhouse gas emissions [1].

In light of these challenges, the valorization of locally available resources represents a promising approach for developing construction materials that are durable, cost-effective, and environmentally sustainable.

Several studies have investigated the use of bivalve shells as a substitute for Portland cement in construction materials. [2] evaluated clam shells, [3] investigated mussel shells, while [4] studied oyster shells as alternative cementitious materials.

Corbula trigona is the most abundant bivalve species in the Ebrié Lagoon (Côte d'Ivoire), with one of the widest geographical distributions, occupying almost the entire lagoon and reaching population densities of up to 1700 individuals/m^2 [5]. Its shells are rich in calcium oxide (CaO) but contain relatively low amounts of silicon dioxide (SiO_2), whereas clay is naturally rich in silica. The complementary chemical compositions of these two materials make them promising candidates for the development of sustainable construction materials.

The main objective is to characterize bivalve shells (*Corbula trigona*), clay and sand for their future use in the design of mortars. Bivalve shells were collected from Jacqueville, located in southern Côte d'Ivoire. The sand was collected from the Ebrié Lagoon, while the clay was sampled in Bingerville, another town situated along the lagoon in southern Côte d'Ivoire.

2. Materials and Methods

2.1. X-Ray Diffraction (XRD)

XRD analyses were performed using a Bruker D8 ADVANCE diffractometer, while mineral identification and quantification were carried out using the FITYK software.

We released the clay minerals in an ultrasonic bath by exposing them to ultrasound for 5 minutes. Then, we added 10% hydrochloric acid (HCl) and gently agitated the sample-water mixture during the treatment to accelerate the release of these minerals. If the water in the beaker is quite cloudy, collect this cloudy

water without the sediment at the bottom. However, if the water remains clear, it is necessary to repeat the ultrasonic treatment. Rinsing is carried out using a centrifuge and aims to remove the mineral salts dissolved in the water to promote better deflocculation of the clay minerals.

To remove these salts, the sample-water mixture must be centrifuged as follows: centrifuge at 3000 rpm for 10 minutes, then repeat the operation until a cloudy solution is obtained. The separation aims to extract only the clay minerals from the cloudy solution. This can be achieved by centrifugation using the following procedure:

- Add a few drops of ammonia to accelerate deflocculation;
- Start centrifugation at 1 minute 06 seconds and 1000 rpm;
- Stop the machine and remove the supernatant.

Next, spread a thin layer of the clay sample onto a glass slide, dry it at 60˚C, and analyze it by XRD. After XRD analysis, impregnate the clay sample with ethylene glycol vapors in a desiccator for at least 12 hours. Then analyze it by XRD. Finally, heat the clay slides to a temperature of 550˚C for 2 hours 30 minutes and perform a final XRD analysis.

2.2. Fourier Transform Infrared Spectroscopy (FTIR)

Fourier Transform Infrared Spectroscopy (FTIR) was used to characterize the clay. This technique is particularly suitable for investigating the local environment of molecular groups whose characteristic vibration frequencies differ significantly from those of the crystal lattice. It complements the mineralogical information obtained by XRD.

FTIR analysis enables the identification of functional groups present in clay minerals. These functional groups exhibit characteristic vibration frequencies and absorb infrared radiation when the frequency of the incident radiation matches their natural vibration frequency, as reported by [6].

2.3. Thermogravimetric Analysis (TG/DTG)

The measuring instrument is a Perkin Elmer ATG 4000. The maximum operating temperature is 1200˚C, and the maximum heating rate is 20˚C/min.

Using tongs, we place a clean, empty crucible, fitted with its metal basket (stirrup), onto the suspension wire.

Once the balance is correctly calibrated, position the sample holder under the crucible and suspension wire, then carefully remove the crucible by lifting the metal basket. Place the sample in the crucible and carefully replace the crucible and metal basket on the suspension wire and wait for stabilization.

2.4. X-Ray Fluorescence Spectroscopy (XRF)

After grinding the samples to obtain a Blaine specific surface area of 3000 cm^2/g, we calcined them at 950˚C ± 25˚C to form beads using 1 g of powder + 8 g of flux (dilithium tetraborate). After bead formation, we sent them to the spectrometer

for oxide analysis.

XRF was performed on bivalve shell powder (*Corbula trigona*), calcined and uncalcined clay, and sand.

2.5. Particle Size Distribution

Sieve analysis consisted of passing the sand sample through a series of standard sieves arranged in descending mesh sizes. Each sieve retained particles larger than its opening while allowing finer particles to pass through. The mass retained on each sieve was measured to determine the particle-size distribution.

The test was conducted in accordance with [7].

2.6. Sand Equivalent Test

The sand equivalent (SE) test was used to evaluate the proportion of clean sand relative to clay-sized particles. According to [8], two 120 g oven-dried sand samples were placed into graduated cylinders containing a standardized solution. One cylinder was used for the visual test and the other for the piston method. The cylinders were shaken for 90 ± 1 cycles within 30 ± 1 seconds and then allowed to stand vertically for 20 minutes.

After sedimentation, the heights of the clay suspension and the sand layer were measured, and the SE and visual sand equivalent (VSE) values were calculated using the standardized equations.

According to [9], sands with an SE value of 80% or higher are classified as very clean sands.

2.7. Bulk Density

Bulk density is defined as the mass of a material divided by the total volume it occupies, including the voids between particles. It is commonly used to evaluate aggregates intended for construction materials.

Bulk density measurements were performed according to [10]. A cylindrical container of known volume was weighed empty (M_1), filled with loose sand without compaction, leveled, and weighed again (M_2). The bulk density was then calculated from the measured mass and container volume.

2.8. Specific Gravity of Sand

The specific gravity (absolute density) of the sand was determined using the pycnometer method in accordance with [11].

A clean and dry pycnometer of known volume was weighed (m_1), filled with oven-dried sand, and weighed again (m_2). Distilled water of known density was then added before recording the final mass (m_3). The particle volume and the specific gravity were subsequently calculated using the standard procedure.

2.9. Fineness Modulus

The fineness modulus (FM) was calculated as one hundredth of the sum of the

cumulative percentages retained on the standard sieves with openings of 0.16, 0.315, 0.63, 1.25, 2.5, and 5 mm, in accordance with [12].

3. Results and Discussion

3.1. Sand

3.1.1. Particle Size Distribution

The particle size distribution of the sand was determined in accordance with [7]. The cumulative retained percentages obtained from the sieve analysis are presented in **Figure 1**.

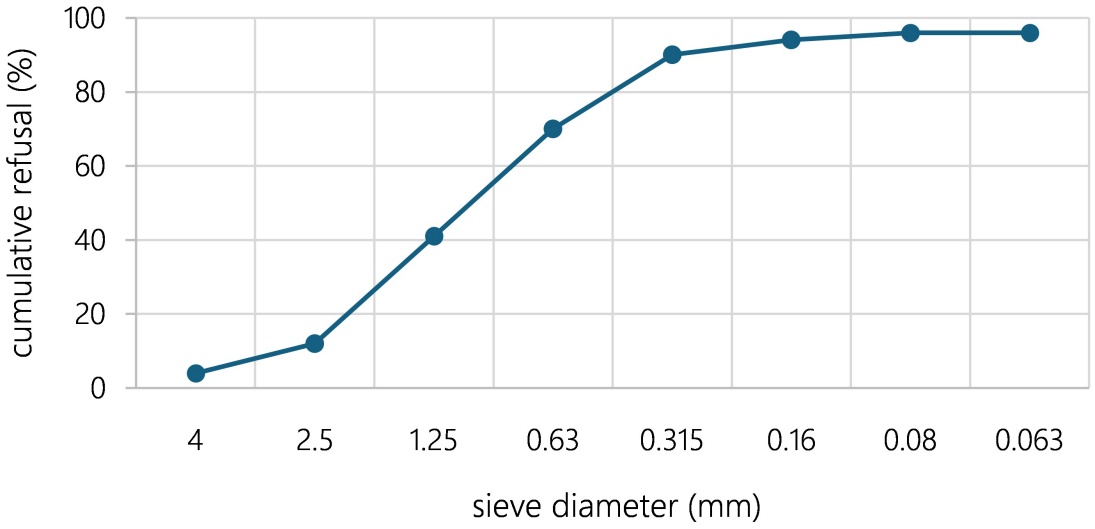

Figure 1. Particle size distribution of the sand.

The results indicate that the sand has a 0/4 grading. According to [13], this grading corresponds to aggregates suitable for mortar production. The calculated fineness modulus (FM) is 3.07, indicating that the material is a slightly coarse sand. Such a grading is generally suitable for mortar production because it contributes to good particle packing and satisfactory mechanical performance.

3.1.2. Sand Equivalent

The results of the sand equivalent test are presented in **Table 1**.

Table 1. Sand equivalent measurement.

	Visual	Piston	Visual	Piston
Tests	N˚1	N˚1	N˚2	N˚2
h (cm)	43	43	43	43
h2		8.6		8.7
h'2	9.7		10	
h1	10		10.3	
ES (%)	ESV1 = 97	ES1 = 86	ESV2 = 97.08	ES2 = 84.46

The average visual sand equivalent (VSE) was 97%, whereas the average sand equivalent (SE) obtained using the piston method was 85%.

According to the classification proposed by [9], sand with an SE value greater than or equal to 80% is classified as very clean sand. Therefore, the tested sand contains only a small proportion of clay-sized particles and is suitable for the manufacture of mortars and concrete.

3.1.3. Bulk Density

The measured bulk density of the sand was 1.54 g/cm^3 (1540 kg/m^3).

According to [10], the typical bulk density of uncompacted construction sand ranges from 1400 to 1600 kg/m^3, whereas compacted sand generally exhibits values between 1600 and 1800 kg/m^3.

The obtained value therefore falls within the normal range for loose construction sand. This result indicates that the sand has a normal packing density and a typical void ratio between particles, making it suitable for mortar and concrete production.

3.1.4. Specific Gravity

The specific gravity of the sand was found to be 2.55 g/cm^3.

Natural siliceous sands generally exhibit specific gravity values ranging from 2.6 to 2.7 g/cm^3, while mixed natural sands usually range between 2.5 and 2.7 g/cm^3.

The measured value therefore falls within the expected range for natural aggregates commonly used in construction materials, confirming the suitability of the sand for mortar production.

3.1.5. X-Ray Fluorescence (XRF) Analysis

The oxide composition of the sand determined by X-ray fluorescence (XRF) is presented in Table 2.

Table 2. Oxide composition of the sand.

Oxide	Na_2O	Al_2O_3	SiO_2	P_2O_5	K_2O	CaO	TiO_2	Cr_2O_3	Fe_2O_3	SrO	Mn_2O_3	PAF
Mass Percentage (%)	0.26	1.54	95.88	0.03	0.38	0.34	0.07	0.13	1.62	0.01	0.10	0.61

The results reveal that the sand is composed predominantly of silicon dioxide (SiO_2), representing approximately 95.88 wt.% of the total oxide composition. Minor amounts of Al_2O_3, Fe_2O_3, Na_2O, K_2O, CaO, TiO_2, Cr_2O_3, SrO, and Mn_2O_3 were also detected.

The high silica content indicates that the aggregate is essentially a siliceous sand. Such mineralogical composition provides good chemical stability and mechanical strength, making the material particularly suitable for the production of construction mortars.

3.2. Clay

3.2.1. X-Ray Diffraction (XRD)

The X-ray diffraction (XRD) pattern of the clay is presented in Figure 2.

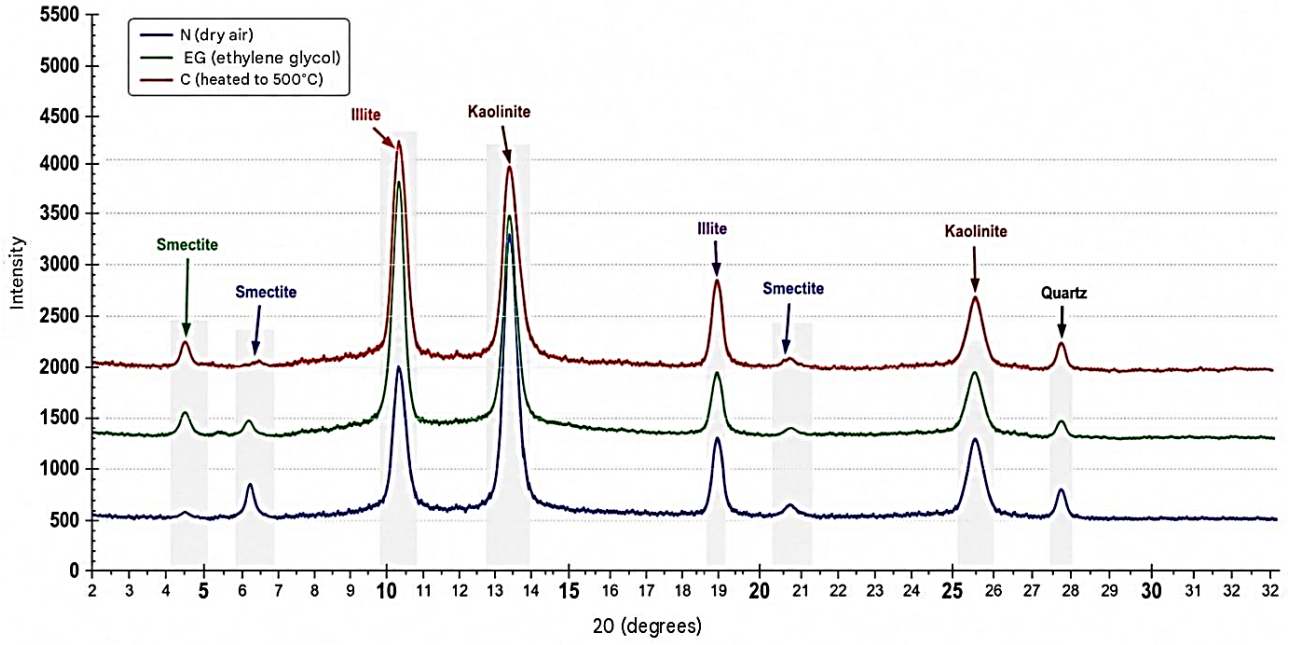

Figure 2. X-ray diffraction (XRD) pattern of the clay.

The XRD analysis indicates that the clay is composed predominantly of kaolinite, followed by illite and smectite, while quartz is present in smaller amounts. The shift of the smectite diffraction peak from approximately 6˚ 2θ to 4˚ 2θ after ethylene glycol treatment confirms the swelling behavior of the smectite phase. Heating the clay to 500˚C results in the progressive destruction of kaolinite, whereas illite and quartz remain stable under these thermal conditions.

3.2.2. Thermogravimetric Analysis (TG/DTG)

The TG/DTG curves of the clay are shown in Figure 3.

An initial endothermic peak is observed between 100˚C and 200˚C, corresponding to a slight mass loss due to the evaporation of water contained in the sample, as demonstrated by [14]. This is followed by a strong endothermic peak in the DTG curve (3.48%) and a significant drop in the ATG curve between 200˚C and 500˚C, corresponding to the dehydroxylation of kaolinite, transforming it into metakaolinite, as described by [15] according to the equation:

$Al_2Si_2O_5(OH)_4 \rightarrow Al_2Si_2O_7 + 2H_2O$

(Kaolinite) (Metakaolinite)

A third phase, characterized by a slight mass loss between 500˚C and 700˚C, likely corresponds to the dehydroxylation of the remaining mass, followed by stabilization above 700˚C.

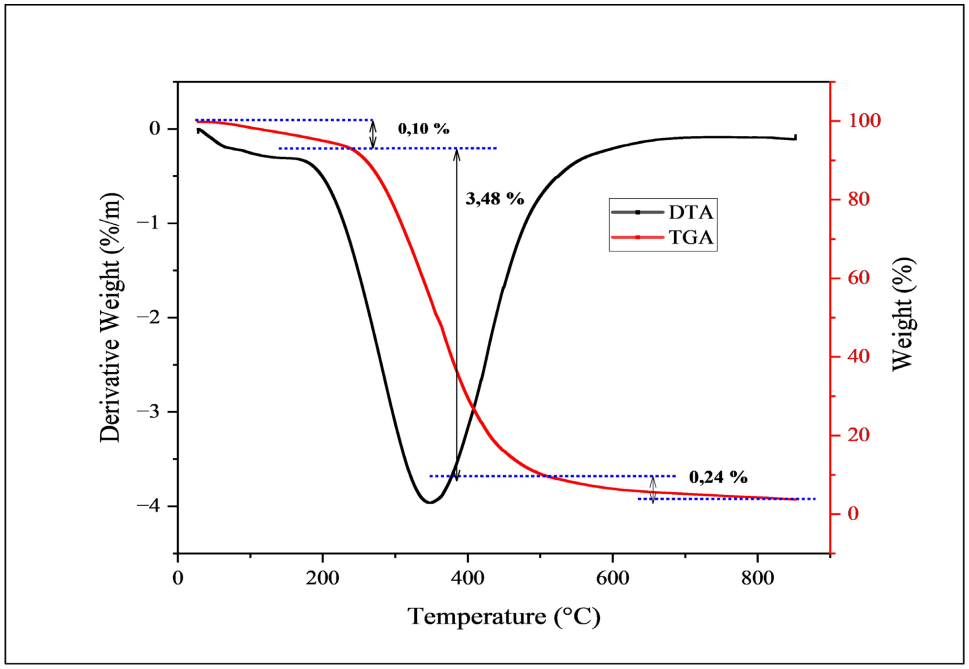

Figure 3. TG/DTG curves of the clay.

3.2.3. X-Ray Fluorescence (XRF) Analysis

The oxide compositions of both the raw and calcined clay are presented in **Table 3** and **Table 4**.

Table 3. Oxide composition of the uncalcined clay.

Oxide	Na_2O	MgO	Al_2O_3	SiO_2	P_2O_5	K_2O	CaO	TiO_2	Cr_2O_3	Fe_2O_3	SO_3	MnO	PAF
Composition (%)	1.97	0.62	16.06	55.82	0.19	1.38	1.97	0.98	0.09	4.69	1.96	0.04	14.13

Table 4. Oxide composition of the calcined clay.

Oxide	Na_2O	MgO	Al_2O_3	SiO_2	P_2O_5	K_2O	CaO	TiO_2	Cr_2O_3	Fe_2O_3	SO3	Mn_2O_3	PAF
Composition (%)	0.10	0.23	28.01	63.51	0.06	1.01	0.36	1.16	0.03	3.27	0.01	0.03	2.5

The raw clay contains mainly SiO_2 (55.82 wt.%) and Al_2O_3 (16.06 wt.%), together with smaller amounts of Fe_2O_3, CaO, MgO, SO_3, K_2O, and P_2O_5.

After calcination at 700˚C, the chemical composition changes significantly. The calcined clay contains 63.51 wt.% SiO_2, 28.01 wt.% Al_2O_3, and 3.27 wt.% Fe_2O_3, with a loss on ignition (LOI) of 2.5 wt.%.

According to the requirements of ASTM C618-05, a pozzolanic material must contain at least 70 wt.% of the combined oxides SiO_2 + Al_2O_3 + Fe_2O_3 and exhibit a maximum loss on ignition (LOI) of 10 wt.%.

The calcined clay satisfies these requirements, with a combined oxide content of 97.78 wt.% and an LOI of 2.5 wt.%. Therefore, this clay can be considered a

pozzolanic material suitable for use as a supplementary cementitious material in Portland cement.

3.2.4. Fourier Transform Infrared Spectroscopy (FTIR)

The FTIR spectrum of the clay is presented in Figure 4.

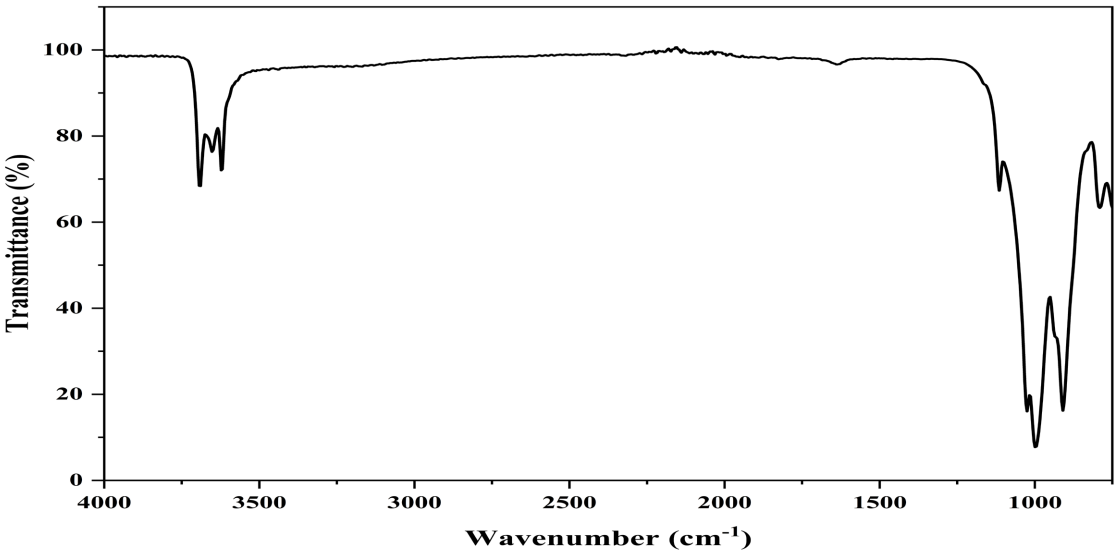

Figure 4. FTIR spectrum of the clay.

The absorption bands observed between 3700 and 3500 cm^{-1} correspond to the stretching vibrations of the internal hydroxyl (OH) groups characteristic of kaolinite.

The absorption band located at approximately 1600 cm^{-1} is attributed to the bending vibration of adsorbed molecular water (H-O-H).

The band around 1000 cm^{-1} is associated with the stretching vibrations of Si-O bonds, while the absorption band between 950 and 900 cm^{-1} corresponds to the deformation vibrations of Al-OH groups.

Finally, the absorption band between 800 and 700 cm^{-1} is assigned to the Si-O-Al vibration, confirming the presence of aluminosilicate minerals in the clay.

3.3. Bivalve Shells (*Corbula trigona*)

3.3.1. X-Ray Fluorescence (XRF) Analysis

The shells of bivalve (*Corbula trigona*) were rinsed with tap water, air-dried, and then ground for 3 hours in a ball mill. They were then sieved through an 80-micrometer mesh before XRF analysis. The results are shown in Table 5.

Table 5. Oxide composition of uncalcined bivalve (*Corbula trigona*) shells.

Oxide	Na_2O	MgO	Al_2O_3	SiO_2	P_2O_5	SO_3	K_2O	CaO	TiO_2	Fe_2O_3	SrO	Mn_2O_3	PAF
Composition (%)	0.23	0.01	0.60	1.86	0.04	0.10	0.02	52.76	0.02	0.74	0.21	0.03	43.72

The bivalve shells were first rinsed with tap water, air-dried, and then calcined in a Nabertherm muffle furnace, with a temperature range of 200˚C - 1200˚C, for 2 hours at 900˚C. The XRF analysis results are shown in Table 6.

Table 6. Oxide composition of bivalve (*Corbula trigona*) shells calcined at 900˚C.

Oxide	Na_2O	MgO	Al_2O_3	SiO_2	P_2O_5	SO_3	K_2O	CaO	TiO_2	Fe_2O_3	SrO	Mn_2O_3	PAF
Composition (%)	0.26	0.01	0.78	2.22	0.05	0.11	0.04	72.23	0.03	1.05	0.28	0.03	23.12

The results show that the shells are composed predominantly of CaO (52.76 wt.%), confirming their calcareous nature. Minor amounts of SiO_2 (1.86 wt.%), Al_2O_3 (0.60 wt.%), Na_2O (0.23 wt.%), Fe_2O_3 (0.74 wt.%), MgO (0.01 wt.%), TiO_2 (0.02 wt.%), SrO (0.21 wt.%), Mn_2O_3 (0.03 wt.%), K_2O (0.02 wt.%), and P_2O_5 (0.04 wt.%) were also detected. The loss on ignition (LOI) was 43.72 wt.%.

The high calcium oxide content indicates that *Corbula trigona* shells constitute a calcium-rich raw material with significant potential for use in the development of cementitious and construction materials.

3.3.2. Thermogravimetric Analysis (TG/DTG)

The TG/DTG curves of the *Corbula trigona* bivalve shells are presented in Figure 5.

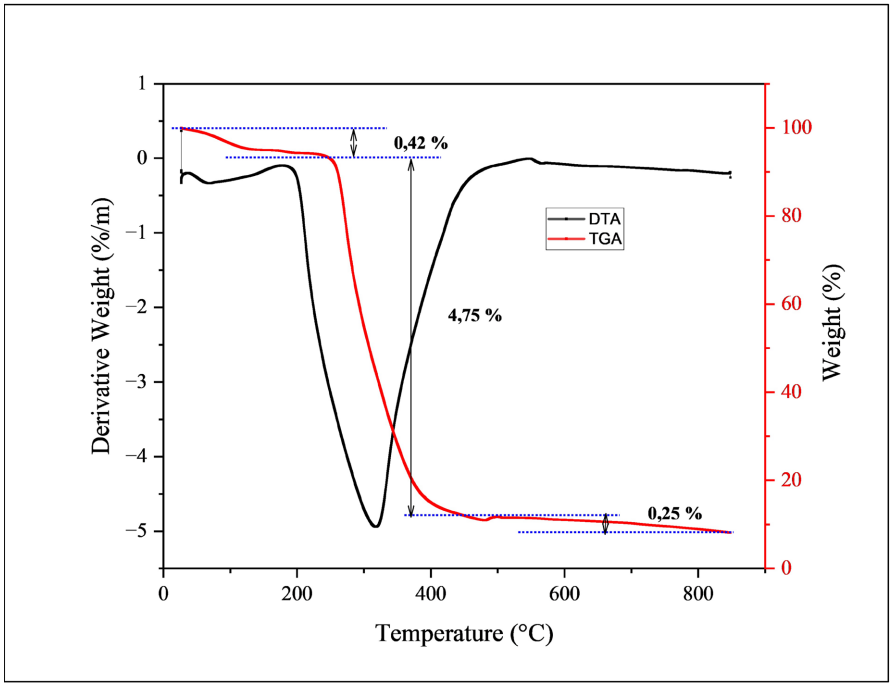

Figure 5. TG/DTG curves of the *Corbula trigona.*

An initial mass loss occurs between 50˚C and 200˚C, explained by the loss of residual water. Then, between 200˚C and 500˚C, a significant mass loss (ATG) is

observed, accompanied by a strong endothermic peak in DTG of 4.75%. This corresponds to the decomposition of calcium carbonate, as demonstrated by [16] according to the equation: $CaCO_3 \rightarrow CaO + CO_2$.

Between 500˚C and 800˚C, a slight mass loss is observed, which may reflect the decomposition of residual calcium carbonate [17]. Above 800˚C, the sample stabilizes.

Conflicts of Interest

The authors declare no conflicts of interest regarding the publication of this paper.

References

[1] ONU Changements climatiques infos (2018) L'association mondiale du ciment appelle le secteur à agir d'urgence en faveur du climat. CCNUCC. https://unfccc.int/fr/news/l-association-mondiale-du-ciment-appelle-le-secteur-a-agir-d-urgence-en-faveur-du-climat

[2] Djeballi, C. (2020) Valorisation des coquilles de palourde et du sable de dragage dans les matériaux cimentaires. http://hdl.handle.net/11143/17853

[3] EL Biriane, M., Barbachi, M. and Imad, A. (2019) Utilisation des coquilles de moules dans les bétons et les mortiers. 14*e congrès de mécanique*, Rabat, 16-19 avril 2019.

[4] Zhong, B.Y., Zhou, Q., Chan, C.F. and Yu, Y. (2012) Structure and Property Characterization of Oyster Shell Cementing Material. *Chinese Journal of Structural Chemistry*, 31, 85-92.

[5] Binder, E. (1968) Répartition des mollusques dans la lagune Ebrié (Côte d'ivoire). *Cahiers O.R.S.T.O.M. Série Hydrobiologie*, **2**, 3-34. https://horizon.documentation.ird.fr/exl-doc/pleins_textes/cahiers/hydro-bio/18059.pdf

[6] Sanou, I. (2017) Influence du mélange ciment-pouzzolane sur quelques propriétés physiques et mécaniques des adobes. Thèse de Doctorat, Université Joseph KI-ZERBO.

[7] AFNOR (1997) NF EN 933-1. Norme Européenne, norme Française d'essais pour déterminer les caractéristiques géométriques des granulats.

[8] AFNOR (2012) NF EN 933-8. Norme Européenne, norme Française d'essai equivalent de sable.

[9] Dreux, G. (1964) Contribution à l'étude de l'influence de la propreté du sable sur les qualités du béton. *Annales de l'Institut Technique du Bâtiment et des Travaux Publics*, No. 198.

[10] AFNOR (1998) NF EN 1097-3. Norme Européenne, norme Française de méthode pour la détermination de la masse volumique en vrac et de la porosité intergranulaire.

[11] AFNOR (2022) NF EN 1097-6. Norme Européenne, norme Française pour la détermination de la masse volumique réelle et du coefficient d'absorption d'eau.

[12] AFNOR (2003) NF EN 13139 P18-540. Norme Européenne, Norme Française granulats pour les Granulats.

[13] AFNOR (2011) NF P18-545. Norme Française pour Granulats-éléments de définition, conformité et codification.

[14] Joseph, S.O., Olalekan, D.A., Moses, A.O., Isah, A.G. and Sallau, A.A. (2023) Characterization of Kaolin Deposits in Kutigi, Niger State, Northern Nigeria. *Walisongo Journal of Chemistry*, **6**, 134-142. https://doi.org/10.21580/wjc.v6i2.17283

[15] Lemaitre, J., Léonard, A.J. and Delmon, B. (1982) Le mécanisme de la transformation thermique de la métakaolinite. *Bulletin de Minéralogie*, **105**, 501-507. https://doi.org/10.3406/bulmi.1982.7572

[16] Naemchanthara, K., Meejoo, S., Onreabroy, W. and Limsuwan, P. (2008) Temperature Effect on Chicken Egg Shell Investigated by XRD, TGA and FTIR. *Advanced Materials Research*, **55**, 333-336. https://doi.org/10.4028/www.scientific.net/amr.55-57.333

[17] Elejalde-Cadena, N.R., Hernández-Juárez, E., Tapia-Mendoza, E., Moreno, A. and Bucio, L. (2025) Structural Insights into Ratite Birds and Crocodile Eggshells for Advanced Biomaterials Design. *ACS Omega*, **10**, 5064-5079. https://doi.org/10.1021/acsomega.4c10850